

Accelerated biological aging in people with Down syndrome with full and segmental trisomy 21 begins in childhood as revealed by immunoglobulin G glycosylation

Ana Cindric

Genos Glycoscience Research Laboratory <https://orcid.org/0000-0002-0935-0192>

Franco Vuckovic

Genos Glycoscience Research Laboratory

David Koschut

Agency for Science, Technology, and Research (A*STAR) <https://orcid.org/0000-0003-2204-5165>

Vincenzo Borelli

Department of Experimental, Diagnostic and Specialty Medicine, University of Bologna

Julija Juric

Genos Glycoscience Research Laboratory

Maja Pucic-Bakovic

Genos Glycoscience Research Laboratory

Anita Slana

Genos Glycoscience Research Laboratory

Helena Deris

Genos Glycoscience Research Laboratory

Azra Frkatović

Genos Glycoscience Research Institute <https://orcid.org/0000-0002-0751-4421>

Aoife Murray

The Blizard Institute, Barts & The London School of Medicine, Queen Mary University of London

<https://orcid.org/0000-0002-4780-3957>

Ivan Alic

QMUL <https://orcid.org/0000-0002-8125-8198>

Jurgen Groet

The Blizard Institute, Barts & The London School of Medicine, Queen Mary University of London

Niamh O'Brien

The Blizard Institute, Barts & The London School of Medicine, Queen Mary University of London

Drazen Petrovic

Genos Glycoscience Research Laboratory

Sarah Hamburg

Division of Psychiatry, University College London

Carla Startin

Division of Psychiatry, University College London

Rosalyn Hithersay

Division of Psychiatry, University College London

Hana D'Souza

Centre for Brain and Cognitive Development, Birkbeck, University of London

LonDownS Consortium

Division of Psychiatry, University College London

Tim Spector

KCL

Dinko Mitrecic

Croatian Institute for Brain Research, School of Medicine, University of Zagreb

Mijana Kero

Department of Medical Genetics, Children's Hospital Zagreb, Centre of Excellence for Reproductive and Regenerative Medicine, School of Medicine, University of Zagreb

Ljubica Odak

Department of Medical Genetics, Children's Hospital Zagreb, Centre of Excellence for Reproductive and Regenerative Medicine, School of Medicine, University of Zagreb

Ingeborg Barisic

Department of Medical Genetics, Children's Hospital Zagreb, Centre of Excellence for Reproductive and Regenerative Medicine, School of Medicine, University of Zagreb

Michael Thomas

Centre for Brain and Cognitive Development, Birkbeck, University of London

Andre Strydom

Department of Forensic and Neurodevelopmental Sciences, Institute of Psychiatry, Psychology and Neuroscience, King's College London

Anne-Sophie Rebillat

Institut Jerome Lejeune

Claudio Franceschi

University of Bologna <https://orcid.org/0000-0001-9841-6386>

Gordan Lauc

University of Zagreb <https://orcid.org/0000-0003-1840-9560>

Jasminka Kristic (✉ jkristic@genos.hr)

Genos Glycoscience Research Laboratory <https://orcid.org/0000-0001-8463-3814>

Dean Nizetic

The Blizzard Institute, Barts & The London School of Medicine, Queen Mary University of London

Keywords:

Posted Date: December 15th, 2021

DOI: <https://doi.org/10.21203/rs.3.rs-1128079/v1>

License:  This work is licensed under a Creative Commons Attribution 4.0 International License.

[Read Full License](#)

Additional Declarations: **Yes** there is potential Competing Interest. Gordan Lauc is the founder and owner of Genos Ltd, a private research organization that specializes in high-throughput glycomic analyses and has several patents in this field. A.Cindric, F.Vuckovic, J.Juric, M.Pucic-Bakovic, A.Slana, H. Deris, A.Frkatovic, D.Petrovic and J.Kristic are employees of Genos Ltd.

Version of Record: A version of this preprint was published at EBioMedicine on July 12th, 2023. See the published version at <https://doi.org/10.1016/j.ebiom.2023.104692>.

Abstract

Cells from people with Down syndrome (DS) show faster accumulation of DNA damage and epigenetic aging marks. Causative mechanisms remain un-proven and hypotheses range from amplified chromosomal instability to actions of several supernumerary chromosome 21 genes. Plasma immunoglobulin G (IgG) glycosylation profiles are established as a reliable predictor of biological and chronological aging. We performed IgG glycan profiling of n=246 individuals with DS (208 adults and 38 children) from three European populations and compared these to age-, sex- and demography-matched general populations. We uncovered very significantly increased IgG glycosylation aging marks associated with DS. Average levels of IgG glycans without galactose (G0) and those with two galactoses (G2) as a function of age in persons with DS corresponded to levels detected in 19 years older euploid individuals. Some aging marks were significant already in children with DS. Remarkably, the IgG glycan profiles of a child with segmental duplication of only 31 genes on chromosome 21 had values similar to those of age-matched DS children, outside the normal children's range. This is the first non-epigenetic evidence of accelerated systemic biological aging in DS, suggesting it begins very early in childhood. It points to a causative contribution of the overdose of genes in a short segment of chromosome 21, not previously linked to accelerated aging, opening a route to discovery of hitherto unrecognised mechanisms.

Introduction

Down syndrome (DS) is an aneuploid condition caused by full or partial trisomy 21 (T21) ^{1,2}. Besides characteristic features resulting from facial, skeletal, muscular and soft-tissue changes, it is the most common genetic cause of intellectual disability and early-onset Alzheimer's disease (AD) and dementia ³. Life expectancy of adults with DS has increased in societies with better access to healthcare to an average of late 60s and 70s, and Alzheimer's dementia (AD) was recognized as the leading cause of death in all individuals with DS older than 35 ⁴. In addition to AD, signs of aging-related reduction in tissue regenerative capacity (such as alopecia, xerosis, delayed wound healing, chronic periodontitis, osteoporosis and immunosenescence) are often seen in DS earlier than in age-matched euploid individuals ⁵⁻⁸. While increased incidence and earlier onset of AD in DS is clearly caused by the triplication of the chromosome 21 gene for amyloid precursor protein (*APP*) ^{9,10}, the explanations for all other aging-related phenomena are less well understood ^{11,12}. Signs of increased DNA damage and/or hypo-functioning DNA-damage-repair (DDR) mechanisms were seen in DS neurons ^{13,14}, fibroblasts ¹⁵⁻¹⁷, lymphocytes ¹⁸⁻²¹ and gingival cells ^{7,22}, while as well being partially reproduced in brains ²³ and hematopoietic stem cells ²⁴ of DS mouse models. These phenomena were observed very early in development, including in fetal DS fibroblasts and amniocytes ^{17,25}.

Immunoglobulin G (IgG) is a protein crucial for the immune response that contains one highly conserved N-glycosylation site. Though it only contains one glycosylation site, variations in the glycans attached to

IgG are known to cause major structural and functional changes (reviewed in ²⁶) and have been correlated with many physiological states and diseases ²⁷. It was recently established that IgG glycosylation is a biomarker of both chronological and biological aging ²⁸. A study of IgG glycosylation in 5,117 individuals from four European populations has revealed very extensive and complex changes in IgG glycosylation with age. The combined index composed of only three IgG glycans (one glycan without galactose and two glycans with two galactoses) explained up to 64% of variance in age, considerably more than other biomarkers of age including telomere lengths. The remaining variance in these glycans strongly correlated with physiological parameters associated with general health status ²⁸.

Evidence for accelerated chronological aging defined by the DNA-methylation based “epigenetic clock” has been recorded for some cell types in DS ²⁹, but the extent to which this affects the biological aging and its relationship to co-morbidities of DS remains unclear. With this as aim, we set up a systematic analysis of IgG glycosylation patterns in three cohorts of adults with DS that were also characterized for the most common comorbidities: Alzheimer’s dementia, thyroid dysfunction, other autoimmune diseases, and frequent respiratory tract infections. The comparison with IgG glycosylation profiles of healthy euploid individuals matched for age, sex and (where possible) demography, was performed on each DS cohort as a whole, and separately for the sub-cohorts with, and those without, specific comorbidities.

Results

We analysed the glycosylation profiles of immunoglobulin G (IgG) in three independent European cohorts of people with DS from France, Italy and the UK. The basic characteristics of the cohorts are given in **Table 1**. IgG glycosylation was analysed using a well-established reliable liquid chromatography method for IgG N-glycan analysis with confirmed reproducibility and robustness ^{30,31}, and which has already been successfully employed to detect significant changes in glycosylation in many different diseases (such as COVID-19 ³², thyroid disease ³³, multiple sclerosis ³⁴, rheumatoid arthritis ³⁵, cardiovascular disease ³⁶ and systemic lupus erythematosus ³⁷). IgG glycans were separated into 24 chromatographic peaks (GP1-GP24) and glycans corresponding to each individual peak are shown in **Figure 1**. Statistical analysis was performed on 22 directly measured glycan peaks because peaks GP20 and GP21 were excluded from the analysis as described in the Methods section. In addition, structurally similar glycans which share a particular characteristic (absence of galactose (G0), presence of one galactose (G1), two galactoses (G2), sialic acid (S), core fucose (F) or bisecting N-acetylglucosamine (GlcNAc) (B)) were grouped together to form so-called derived glycan traits (see Methods section for details) and were then also included in a separate statistical analysis.

Comparison of IgG glycosylation between persons with Down syndrome and age- and sex-matched healthy controls

We examined the existence of differences in IgG glycosylation between adults with DS and healthy subjects from the general population matched for age, sex and demography (except in the case of the DS cohort from France (see **Methods**)). We observed a significant difference in relative abundances of 14 out of 22 directly measured IgG glycans between persons with DS and matched controls, shifting in the same direction in all three examined cohorts (**Supplementary Figure 1** and **Supplementary Table 1**). Relative abundances of seven additional directly measured IgG glycans were found to be different between persons with DS and controls in (any) two out of three analysed cohorts. Further meta-analysis of all three cohorts showed a significant difference in relative abundances of all 22 analysed IgG glycans between persons with DS and controls (**Supplementary Table 1**). Comparison of the derived IgG glycan traits between persons with DS and matched controls from the general population revealed a higher level of IgG glycans without galactose (G0) and IgG glycans with core fucose (F) in persons with DS (**Figure 2** and **Supplementary Table 1**). At the same time, the level of IgG glycans with two galactoses (G2) and IgG glycans with sialic acid(s) (S) were lower in persons with DS compared to healthy controls. These observations were replicated independently in each of the three cohorts (**Figure 2** and **Supplementary Table 1**). When all three cohorts were combined in the meta-analysis, the level of IgG glycans with one galactose (G1) was also found to be significantly lower in persons with DS than in controls (**Supplementary Table 1**). Levels of two major glycans that make up the G1 IgG glycan trait, glycans corresponding to peaks GP8 and GP9 (**Figure 1**), showed the opposite direction of changes in persons with DS (i.e., the level of IgG glycan GP8 was higher whereas the level of GP9 IgG glycan was lower in persons with DS when compared to controls) (**Supplementary Table 1**). However, the effect size of the difference in glycan levels between DS and controls was higher for GP9 IgG glycan (decreased in DS compared to controls) than for GP8 IgG glycan (increased in DS compared to controls) (**Supplementary Table 1**).

In the Italian DS cohort for 35 individuals with DS, samples from their corresponding non-DS siblings were also available. Glycosylation profiles of IgG of paired samples were analysed and compared, as this provided a comparison between two populations most similar with respect to genotype, environment and sample collection/handling history. We found that nine directly measured IgG glycans and three derived IgG glycan traits differed significantly between persons with DS and their non-DS siblings (**Supplementary Figure 2**, **Supplementary Figure 3** and **Supplementary Table 2**). More specifically, levels of G0, F, and B IgG glycans were all increased in individuals with DS compared to their non-DS siblings. Although the level of G2 IgG glycans was found to be significantly decreased in Italian subjects with DS when compared to non-DS controls from the general population (unrelated control group), only a nominally statistically significant decrease ($p=0.053$) in the level of G2 glycans was observed when individuals with DS from the Italian cohort were compared to their unaffected siblings. This was probably due to lower statistical power in the case of sibling pairs (35 sibling pairs vs. approximately 55 matched DS and unrelated control pairs) (**Table 1**, **Supplementary Figure 3** and **Supplementary Table 2**).

The association of IgG glycosylation with comorbidities common in persons with Down Syndrome

The prevalence of specific comorbidities such as Alzheimer's dementia³⁸, frequent infections¹² and autoimmune thyroid disease³⁹ is high in persons with DS. Also, in addition to high prevalence of thyroid disease, some other autoimmune diseases such as celiac disease and type 1 diabetes mellitus are increased in rates in persons with DS³⁹. These diseases were also previously reported to have an altered IgG glycosylation pattern²⁷. This raised the possibility that differences in IgG glycosylation observed between persons with DS and controls might not be associated with DS itself, but that observed differences could be attributed to additional diseases occurring in persons with DS. To explore this, we divided persons with DS into those with and without a certain comorbidity. To distinguish the effect of DS on IgG glycosylation profile from the effects of comorbidities, we firstly compared a group of people with DS without a certain comorbidity to a group of healthy, non-DS individuals from the general population. We found that the levels of G0 and F IgG glycans were increased whereas the levels of G2 and S IgG glycans were decreased in the sub-cohort of DS without any diagnosed autoimmune disease as well as in the sub-cohort of DS without known autoimmune thyroid disease compared to control subjects (**Figure 3** and **Supplementary Table 3**). The same groups of IgG glycans (G0, F, G2 and S), as shown in the case of DS without autoimmune conditions, were also found to be significantly different in the sub-cohort of DS without dementia as well as the group of DS without frequent infections compared to the control group (**Supplementary Figure 4**, **Supplementary Figure 5** and **Supplementary Table 3**). Additionally, the level of G1 IgG glycans was found to be significantly decreased in the group of DS without dementia as well as in the group of DS without frequent infections compared to the control group (**Supplementary Table 3**). In summary, for DS without comorbidities, we found nearly identical IgG glycan differences as for the whole (co-morbidity-unfiltered) DS cohorts, proving these alterations are caused by trisomy 21 as a genetic condition, and not as a secondary effect of DS co-morbidities.

Secondly, we explored whether differences exist in IgG glycosylation between DS study participants with and without certain comorbidities. Meta-analysis showed that, compared to DS without autoimmune disease diagnosis, individuals with DS with diagnosed autoimmunity had significantly higher level of G0 IgG glycans (**Figure 3a** and **Supplementary Table 4**). Comparison of samples from people with DS with and without autoimmune thyroid disease, the most common autoimmune disease associated with DS, revealed a higher level of G0 IgG glycans and lower levels of G2 and S IgG glycans in individuals with DS with diagnosed thyroid disease (**Figure 3b** and **Supplementary Table 4**). We observed no significant differences in IgG glycosylation between persons with DS with and without dementia or between DS participants with and without frequent infections (**Supplementary Figure 4**, **Supplementary Figure 5** and **Supplementary Table 4**). Slight differences in distribution of glycan profiles between DS groups with and without dementia that can be observed in **Supplementary Figure 4a** reflected the differences in composition of France and UK populations with respect to age (**Supplementary Figure 4b**). Since both AD and IgG glycans are strongly associated with age, any potential correlations of IgG glycan profiles with dementia itself may be difficult to detect and isolate from the correlation with age. While our study cannot exclude such a correlation, a much larger and more age-homogenous cohort would be required to confirm it.

The relationship between IgG glycosylation and age in persons with Down syndrome

It is known that IgG glycosylation changes as a function of age in individuals from the general population^{28,40}. Our observations of IgG glycosylation in healthy non-DS individuals from the general populations (who served as age-, sex- and, when possible, demography-matched controls for persons with DS) confirmed the previously reported increase in levels of G0 and B IgG as well as decrease in levels of G2 and S IgG glycans with increasing age (**Figure 4** and **Supplementary Table 5**). Next, we wanted to examine whether persons with DS also exhibit changes in levels of IgG glycans with age and, if yes, whether persons with DS show a similar pattern of changes in IgG glycans to that observed in the control group. We found that all derived IgG glycan traits whose levels were found to change with age in the control group, also changed with age in persons with DS (**Figure 4** and **Supplementary Table 5**). Specifically, levels of G0 and B IgG glycans increased with age whereas levels of G2 and S IgG glycans decreased with age in persons with DS. However, contrary to euploid individuals from the general population, persons with DS showed a significant decrease in the level of G1 IgG glycans with age (the results of meta-analysis) (**Figure 4** and **Supplementary Table 5**). Neither persons with DS nor control individuals showed a significant change in the level of F IgG glycans with age.

Following the observation that the levels of several derived IgG glycan traits, namely G0, G2, S and B, change with age in both euploid controls and persons with DS, and that the directions of changes were the same in the control and DS groups, we wanted to determine whether a difference exists in the extent of change in levels of derived IgG glycan traits with age between persons with DS and healthy controls. The shape and slope of plotted age-related glycan trend curves for persons with DS and controls were very similar (**Figure 4**) and statistical analysis showed no difference in the rate of age-dependent changes in the level of derived IgG glycan traits between persons with DS and healthy individuals from the general population (**Supplementary Table 6**). However, the position of curves showing IgG glycan levels as a function of age differed significantly between persons with DS and controls (**Figure 4**). Specifically, we observed that in the case of G0 glycan trait, the level of which was shown to increase with age, the curve that corresponds to persons with DS lay above the curve corresponding to controls, and in the case of G2 glycan trait, whose level was shown to decrease with age, the curve that corresponds to persons with DS lay below the curve corresponding to controls. Signs of premature aging have been described for persons with DS⁴¹. Furthermore, we recently showed that G0 and G2 IgG glycans are good biomarkers of biological age²⁸, that better reflect overall age-related health status of an individual than the purely chronological age does. When we looked at the curve showing the level of G0 IgG glycans as a function of age (**Figure 4**), we determined that, on average, the levels of G0 glycan trait in persons with DS corresponded to levels found in 18.4 years older individuals from the general population (France (FRA) 11.7-12.2 years (average 11.9 years); Italy (ITA) 15.1-20.0 years (average 17.5 years); UK 20.4-31.1 years (average 25.8 years)). Based on the curve showing the level of G2 IgG glycans as a function of age (**Figure 4**), we found that the level of G2 glycans in persons with DS corresponded to levels found in 19.1 years older individuals from the general population (FRA 15.0-17.6 years (average 16.3 years); ITA 17.1-17.9 years (average 17.5 years), UK 22.1-25.1 years (average 23.6 years)).

IgG glycosylation in children with Down syndrome

In the UK DS cohort, samples from 38 children with DS aged between 0.58 and 5.25 years were available. However, for euploid (typically developing healthy children) controls, apart from two samples from 3-year-old children, we only had available samples from children from Croatia aged 4 years and older due to ethical constraints in obtaining samples from healthy babies and very young, healthy children. Therefore, we compared IgG glycosylation in plasma samples obtained from eight children with DS aged around 4 years with IgG glycosylation in plasma samples collected from 11 age-matched healthy children. We observed that 4-year-old children with DS had a higher level of G0 IgG glycans compared to 4-year-old healthy children (**Figure 6a** and **Supplementary Table 7**). An increased level of G0 IgG glycans was also observed in adults with DS (**Figure 2**). In addition, we observed a nominally significant ($p= 0.052$) decrease in the level of G2 IgG glycans in children with DS compared to healthy children (**Figure 6a** and **Supplementary Table 7**).

Typical DS pattern of IgG glycosylation in a child with a segmental duplication of chromosome 21 causing trisomy of only 31 genes

A 2 year-old child from Croatia observed with signs of developmental delay and dysmorphic features in the spectrum of DS (**Figure 5a** and **Supplementary Table 8**) was analysed by karyotyping which showed a normal (euploid) karyotype of 46,XX (**Figure 5b**). On high resolution banding, a small duplication in one copy of the chromosome 21 was observed (**Figure 5b, arrow**). A high resolution SNP-array showed a segmental duplication of 4 Mbp on one chromosome 21 copy, encompassing 31 genes (**Figure 5c,d**), from (and including) DOPEY2, to (and including) PCP4, as the only genomic DNA anomaly. Due to a stretch of fewer informative SNPs for the segment harbouring the genes DOPEY2, MORC3 and CHAF1B, we can only tentatively include these genes in the duplication (in its maximal possible size estimate). Its minimal estimate is for 28 genes, from (and including) CLDN14, to (and including) PCP4. The gene DSCAM is broken in the middle by the duplication breakpoint. This region approximately corresponds to the previous definition of the "Down syndrome Critical Region (DSCR)"^{42,43}, a region on chromosome 21 that was originally thought to be responsible for many features of DS, so we named this sample "Critical Region Only-1 (CRO1)". The values for IgG glycan traits: G0 (higher); G1, G2 and S (lower) for this child (from Croatian) (**Figure 6a, marked as single black cross**) were all outside the range of the euploid 4 year-old children from the Croatian cohort ($n=11$), and clearly segregating with 1 to 5 year-old children with DS on derived glycan trait graphs (**Figure 6a**), as well as on two different ways of calculating the Principal Component Analysis (PCA) using directly measured IgG glycan peak values (GP1-GP24) (**Figure 6b**), or the PCA using derived IgG glycan trait parameters (**Figure 6c**). The values for 4 year-olds with DS are also separately shown as they were the only ones exactly statistically compared to fully age-matched euploid (normal) controls. In this comparison (**Figure 6a**), the CRO1 child gave IgG glycan values clearly more extreme than the mean of the DS group that was statistically significantly different from euploid controls' mean. For the purposes of completeness and exactness of age-matching, we also showed the values for $n=9$ of 2-year-old children with DS, the same age as the child with the segmental duplication (**Supplementary Figure 6**). The data clearly indicate that trisomy of one or more of

chromosome 21 genes in this segment could be sufficient to produce the IgG glycome profile changes observed for DS very early in life.

Discussion

Compared to other biomarkers of aging, IgG glycan profiles were shown to be a more reliable estimator of biological age, explaining up to 64% of the variation in chronological age²⁷. Specifically, IgG structures containing two galactoses (G2) decrease, while IgG structures containing no galactose (G0) increase with age²⁸, whereas the levels of IgG glycans containing one galactose do not change consistently with age, and this glycan trait (G1) was found to be most influenced by the demography factors⁴⁰.

By profiling plasma samples from n=246 individuals (208 adults and 38 children) with DS from three independent European populations, we found that the glycan aging marks identified in euploid populations (decreased G2 and increased G0) were very significantly changed in DS. When comparing DS with age-matched euploid controls, we found that in each of the three populations the G2 and S traits were significantly decreased, while G0 and F were significantly increased in DS. As the Italian DS cohort was controlled against their euploid siblings, and the UK cohort was controlled against age-matched UK euploid individuals, the finding of the exact same comparison results also in the French population (demographically un-matched, as it was controlled against a Croatian cohort) decreases the likelihood of genotypic and geographical factors causing the observed differences. Instead, the data show a robustly accelerated IgG glycan aging pattern driven predominantly by trisomy 21.

For children with DS, we could only make an age-matched statistical comparison with 4-year-olds, due to limited access to euploid children samples. When n=8 children with DS were compared to n=11 euploid children aged 4, a statistically significant increase in G0 and a nominally significant decrease in G2 IgG glycans were observed, showing exactly the same trend as in the adult cohorts. This suggests that the trisomy 21-driven mechanism that causes these accelerated aging-related IgG glycan changes begins very early in childhood.

The general paradigm predicts that aging of the whole organism is the result of a life-long accumulation of damage to macromolecules, triggering epigenetic and secretory changes associated with senescence and loss of replicative potential⁴⁴. In DS, the mechanistic explanations⁴⁴ for increased DNA damage observations range from amplified developmental instability (triggered by a freely segregating extra chromosome)⁴⁵, to increased action of specific genes from chromosome 21⁴⁶. The amplified instability hypothesis posits that the presence of any of the supernumerary chromosomes (irrespective which specific one) leads to non-specific disturbance of chromosome balance, resulting in a disruption of homeostasis⁴⁵. In support of this view: leukocytes from newborns with DS and adult fibroblasts from individuals with DS have elevated rates of acquired random aneuploidy and mosaicism^{19,25,47,48}, and other viable constitutional aneuploidy syndromes and their mouse models show similar rates of chromosomal instability^{49,50}. Also, genetic conditions causing mosaic variegated aneuploidy (MVA)

syndromes accelerate cellular aging by increasing the numbers of aneuploid cells⁵¹. This also boosts the thinking that DS mouse models with freely segregating supernumerary chromosome material can model DS better than segmental duplication models of trisomy^{52,53}. However, chromosomal instability would predict a steeper slope of change for aging markers (G0 and G2) in DS than in euploid controls. This is not observed in our data (**Figure 4**) where the slope of glycan change with age does not differ between DS and controls for any of the three population. The alternative, specific human chromosome 21 gene dosage imbalance explanation for increased DNA damage, has implicated multiple genes: overdose of APP leads to increased production of shorter proteolytic fragments (e.g. Aβ1-42) that accumulate as aggregates toxic to neurons, causing mitochondrial malfunction and increased DNA damage in neuronal nuclei⁵⁴; overdose of Cu/Mg superoxide dismutase SOD1 leads to increased production of hydrogen peroxide that, in the absence of an increased level of glutathione peroxidase or catalase, leads to an increased concentration of hydroxyl radicals (one of the most toxic reactive oxygen species)⁵⁵; overdose of Ubiquitin Specific Peptidase 16 (USP16) over-de-ubiquitinates H2A-K119, decreasing the replicative potential of DS fibroblasts and neural progenitors⁵⁶. Very intriguingly, we demonstrate that blood plasma from a child with DS caused by a short segmental duplication of only 31 genes on chromosome 21 produces the IgG glycan profiles of accelerated aging (G0 higher than the range of euploid controls, and G2 lower than the range of euploid controls), and in the range of other DS 1- to 5-year-olds. When compared to euploid Croatian 4-year-olds, or full trisomy 21 children (DS) from the UK cohort, the profile of this child with segmental trisomy DS clearly mapped with the DS children. This suggests that having a freely segregating extra chromosome is not necessary to cause the changes observed, and that an increased dose of one or more genes in this duplicated segment is sufficient to cause the IgG-glycan-defined hallmarks of accelerated aging in DS, beginning early in childhood. Neither *APP*, nor *SOD1*, nor *USP16* were found in this segmental duplication, and none of the genes in this region have so far been shown to increase DNA damage by their over-expression alone. Among the genes in this segment, the kinase encoded by *DYRK1A* was recently implicated in regulating the repair of DNA breaks caused by ionizing radiation⁵⁷⁻⁵⁹, and this region contains several transcription factors and chromatin modifiers whose individual and interactive roles remain to be studied in more detail, opening up possibilities of yet undiscovered mechanisms contributing in a major way to accelerated aging in DS.

The main limitation of our study is in the relatively small sub-population of DS patients with specific co-morbidities. This potentially prevents the detection of correlations of IgG glycan profiles with certain diseases within the DS cohorts. This is particularly important for AD-dementia correlations. People with DS have a similar curve of positive correlation of the incidence of dementia with age as euploids, but at younger age of onset and with a much increased frequency³. As IgG glycan profiles also change with age in both DS with and without dementia, any additional profile-skewing correlating with dementia is difficult to separate from the effect of age alone, in the sample size we studied. A larger study of older adults with DS would be required to tease out these differences, with uniformly applied criteria for the dementia diagnosis, and with sufficient numbers of those with and without dementia.

For additional discussions on whole plasma proteome glycosylation in DS⁶⁰, IgG glycans with core fucose (F), and IgG glycan profiles for DS with and without co-morbidities, see **Supplementary Discussion**.

In conclusion, we uncover that IgG glycosylation patterns associated with accelerated aging are very significantly pronounced in DS with and without co-morbidities. Nearly identical qualitative and quantitative differences were found in all three adult DS populations studied. This is the first molecular non-epigenetic evidence of extremely accelerated systemic biological aging, as a DS phenotype. Epigenetic clock CpG-island signatures of accelerated aging have been previously observed in the blood and brain tissues of DS individuals²⁹. For future research, it would be interesting to study the relationship between epigenetic and glycomic markers of aging. Importantly, some of the N-glycomic aging-marks are already significant in children with DS born with full trisomy 21, or even (in one case) partial trisomy of less than 15% of chromosome 21 gene content (only 31 genes). Interestingly, none of these genes were previously causatively associated with accelerated aging, opening up possibilities for hitherto overlooked causative mechanisms.

Methods

Human samples

This study was based on banked plasma samples obtained from three European cohorts of persons with DS:

A) DS cohort from France

Plasma samples from 98 adult individuals with Down syndrome aged 30 to 67 years (median 46 years) were provided by Jérôme Lejeune Institute in Paris. DS samples in the French cohort were stratified for the presence or absence of dementia, autoimmune diseases (type of autoimmune disease was also specified) and frequent infection. An age- and sex-matched control group of plasma samples from 109 healthy individuals aged 22 to 67 years (median 46 years) was selected from the Split cohort which contains samples from individuals from the Croatian city of Split collected through the “10,001 Dalmatians” project^{61,62}.

B) DS cohort from Italy

Plasma samples from 57 adult individuals with Down syndrome aged 22 to 66 years (median 36 years) from the Italian DS cohort were used in this study. Individuals with DS from the Italian cohort were stratified for the presence or absence and type of autoimmune diseases and frequent infection. Plasma samples from 53 healthy adult individuals aged 22 to 66 years (median 38 years) of Italian ethnicity, selected from banked samples collected through the “PainOmics” project⁶³, served as control samples. In addition, plasma samples from 35 individuals with DS (ages 10-58 years, median age 26 years) and 35 of their healthy siblings (ages 9-52 years, median age 31 years) were obtained from the Italian DS cohort

and analysed in this study. These 35 sibling pairs were recruited in the Emilia-Romagna region (Bologna and Ferrara provinces) in Italy.

C) DS cohort from the UK

Plasma samples from 53 adult individuals with Down syndrome aged 22 to 73 years (median 49 years) from the London Down Syndrome Consortium (LonDownS) cohort were used in this study. DS samples in the UK cohort were stratified for the presence or absence of dementia, autoimmune diseases (type of autoimmune disease was also specified) and frequent infection. Control plasma samples were selected from the TwinsUK cohort which is the UK's largest adult twin registry and contains over 14,000 twins⁶⁴. In total, samples from 42 individuals aged 22 to 82 years (median age 47 years) from the TwinsUK cohort were included in this study. Individuals from the TwinsUK cohort have been shown to have comparable disease-related, lifestyle and anthropomorphic characteristics to those of age-matched individuals from the general UK population⁶⁵. In addition, 38 plasma samples from children with DS with age ranging from 0.58 years to 5.25 years from the LonDownS Consortium cohort were analysed in this study. Among these were eight samples obtained from around 4-year-old DS children (three boys and five girls, ages 3.58-4.17 years). Plasma samples from 17 healthy control children who were from 3 to 5 years old were provided by Children's Hospital Srebrnjak (CHS) in Zagreb, Croatia. These control children samples were collected through the "ATOPICA" project at CHS, as previously described⁶⁶. Among these were 11 samples obtained from healthy 4-year-old children (three boys and eight girls).

D) CRO1 partial trisomy

The sample CRO1 was obtained from a 2-year-old child, having observed the clinical features of DS. After finding a normal number of chromosomes, high-resolution banding cytogenetic analysis, followed by genomic DNA analysis using CGH array, confirmed the presence of a small segmental duplication in 21q22. This duplication was fine-mapped by a SNP array on an Illumina OmniExpress v1.1 chip. Analysis was performed and figures were generated using GenomeStudio 2.0 software. Following the list of features reported for other partial trisomy 21 cases⁶⁷, the clinical observations were subsequently followed up in greater detail (summarized in **Supplementary Table 8**).

This study was performed in accordance with the Helsinki declaration. Informed consent was obtained from all individual participants included in the study or from the participant's parents or guardians. Ethical approvals were obtained by relevant ethics committees: for DS cohort from the Institute Jérôme Lejeune in Paris, France approval was obtained from the Ministry of Higher Education, Research and Innovation for biobanking activities (AC-2015-2579), and for human samples exportation (IE-2015-814); for Italian cohort of Down syndrome ethical approval was obtained from the local Ethical Committee (S. Orsola Hospital, University of Bologna); for LonDowns cohort ethical approval was obtained from the North West Wales National Health Service (NHS) Research Ethics Committee (13/WA/0194); "10,001 Dalmatians" study was approved by Ethical Board of the Medical School, University of Split, Croatia;

“PainOmics” study was approved by Ethical Committee of University of Parma (UNIPR), Italy and Fondazione IRCCS Policlinico San Matteo Hospital (OSM), Italy; the TwinsUK study was approved by Westminster Research Ethics Committee; “ATOPICA” study was approved by Children’s Hospital Srebrnjak (CHS) Ethics Committee; for the CRO1 child, the study was approved by the Ethical Research Committee of the Children’s Hospital Zagreb (University of Zagreb, School of Medicine). To ensure a blinded study, the plasma samples were coded by number or by combination of letters and numbers.

Experimental design: randomization, blocking and used standards

Plasma samples from DS individuals and healthy individuals which served as controls were randomized across seven 96-well collection plates. To ensure that each of the seven plates had the same age distribution, sex ratio and ratio of persons with DS and controls as the entire collection of samples and also to ensure an approximately equal number of individuals from each individual cohort on each plate, blocking was performed. In addition to plasma samples from individuals with DS and healthy controls, each plate contained 3-5 wells loaded with human plasma which served as a standard and was obtained from the Croatian National Institute of Transfusion Medicine. One well on each plate contained no plasma and served as a negative control sample. The randomization and blocking methods used in this study are described more precisely in ⁶⁸.

Immunoglobulin G (IgG) isolation

Plasma samples were vortexed after thawing and centrifuged at 12,100 g for 3 min or 5,000 g for 10 min. Then, 100 µL of each plasma sample was aliquoted to 1 mL 96-well collection plates (Waters, Milford, MA, USA) following a predetermined experimental design described above. Plasma samples were diluted with 700 µL of PBS, pH 7.4, and filtered through a 0.45 µm GHP filter plate (Pall Corporation, Ann Arbor, MI, USA). IgG was isolated from plasma samples by affinity chromatography using 96-well monolithic plates with bound Protein G (BIA Separations, Ajdovščina, Slovenia) as described previously ⁶⁹. Following IgG isolation, IgG concentrations were measured at 280 nm using a NanoDrop spectrophotometer (NanoDrop 8000, Thermo Scientific, USA).

IgG N-glycan release, labelling and clean-up

The whole procedure was performed as described previously ³¹. Briefly, 300 µL of IgG eluates were dried in a vacuum centrifuge. After drying, IgG was denatured with sodium dodecyl sulphate (SDS) (Invitrogen, Carlsbad, CA, USA) and a 10 min incubation at 65 °C. The excess of SDS was neutralized with Igepal-CA630 (Sigma-Aldrich, St. Louis, MO, USA). N-glycans were released from IgG by overnight digestion with PNGase F (Promega, Madison, WI, USA). The released IgG N-glycans were labelled with 2-

aminobenzamide (2-AB, Sigma-Aldrich, St. Louis, MO, USA). Free label and reducing agent were removed from the samples using hydrophilic interaction liquid chromatography solid-phase extraction (HILIC-SPE) on a 0.2 μm GHP filter plate (Pall Corporation, Ann Arbor, MI, USA). IgG N-glycans were eluted with ultrapure water and stored at $-20\text{ }^{\circ}\text{C}$ until use.

Ultra-High-Performance Liquid Chromatography (UHPLC)

Fluorescently labeled N-glycans were separated by hydrophilic interaction chromatography (HILIC) on a Waters Acquity UPLC instrument (Milford, MA, USA) consisting of a quaternary solvent manager, sample manager and a FLR fluorescence detector set with excitation and emission wavelengths of 250 and 428 nm, respectively. The instrument was under the control of Empower 3 software, build 3471 (Waters, Milford, MA, USA). Labeled N-glycans were separated on a Waters BEH Glycan chromatography column, $100 \times 2.1\text{ mm}$ i.d., $1.7\text{ }\mu\text{m}$ BEH particles, with 100 mM ammonium formate, pH 4.4, as solvent A and ACN as solvent B. The separation method used a linear gradient of 75–62% ACN (v/v) at flow rate of 0.4 mL/min over 27 min. Samples were maintained at $10\text{ }^{\circ}\text{C}$ before injection and the separation temperature was $60\text{ }^{\circ}\text{C}$. The system was calibrated using an external standard of hydrolyzed and 2-AB-labeled glucose oligomers from which the retention times for the individual glycans were converted to glucose units (GU). Data processing was performed using an automatic processing method with a traditional integration algorithm, after which each chromatogram was manually corrected to maintain the same intervals of integration for all the samples. All chromatograms were separated in the same manner into 24 peaks (GP1 – GP24) as previously reported⁶⁹. The amount of glycans in each peak was expressed as a percentage of total integrated area (% area). To confirm that glycan structures found in each of the 24 peaks are those reported by⁶⁹, GU values of each peak were compared to the reference values in the “GlycoStore” database available at <https://glycostore.org/>. All glycan structures were further confirmed with exoglycosidase digestions. The following enzymes, all purchased from New England Biolabs (NEB, Ipswich, MA, USA) were used for digestions: α 2-3,6,8,9 Neuraminidase A, β 1-4 Galactosidase S, β 1-3 Galactosidase, β -N-Acetylglucosaminidase S, α 1-2,4,6 Fucosidase O. Aliquots of the 2-AB labelled glycan pool were dried down and digested according to the manufacturer's protocol. After overnight incubation at $37\text{ }^{\circ}\text{C}$, enzymes were removed by filtration through AcroPrep 96 Filter Plates, 10K (Pall Corporation, Ann Arbor, MI, USA). Digested glycans were then separated by HILIC-UHPLC for comparison against undigested glycans.

Statistical analysis

To remove experimental variation from measurements, normalization and batch correction were performed on UHPLC glycan data. To make measurements across samples comparable, normalization by total area was performed where peak area of each of 24 glycan structures was divided by total area of the corresponding chromatogram. Prior to batch correction, normalized glycan measurements were log

transformed due to right-skewing of their distributions and multiplicative nature of batch effects. Batch correction was performed on log-transformed measurements using the ComBat method (R package *sva*), where technical source of variation (which sample was analysed on which plate) was modelled as batch covariate. To get measurements corrected for experimental noise, estimated batch effects were subtracted from log-transformed measurements. Glycan peaks 20 and 21 (GP20 and GP21) were not well separated in UHPLC glycan profiles of samples from the fourth and fifth plates. Therefore, these two peaks were excluded from statistical analysis and derived trait calculations. In addition to 22 directly measured IgG glycans (glycan peaks), six derived traits were calculated from the directly measured glycans. These derived traits average glycosylation features across different individual glycan structures and are consequently more closely related to individual enzymatic activities and underlying genetic polymorphisms. Formulas used for the calculation of derived IgG glycan traits were as follows: IgG glycans without galactose G0 total = GP1 + GP2 + GP3 + GP4 + GP6; IgG glycans with one galactose G1 total = GP7 + GP8 + GP9 + GP10 + GP11; IgG glycans with two galactoses G2 total = GP12 + GP13 + GP14 + GP15, IgG glycans with sialic acid(s) S total = GP16 + GP17 + GP18 + GP19 + GP22 + GP23 + GP24; IgG glycans with core fucose F total = GP1 + GP4 + GP6 + GP8 + GP9 + GP10 + GP11 + GP14 + GP15 + GP16 + GP18 + GP19 + GP23 + GP24; IgG glycans with bisecting GlcNAc B total = GP3 + GP6 + GP10 + GP11 + GP13 + GP15 + GP19 + GP22 + GP24.

Differences in N-glycosylation of IgG between individuals with DS and healthy controls were analysed using a general linear model. Age and gender variables were included in the model to control for their effects. The general linear model was also used to determine whether associations exist between IgG N-glycome and various clinical variables (e.g., autoimmunity, dementia, etc.) within the DS group. Differences in IgG N-glycome between individuals with DS and their siblings were analysed using the linear mixed effects model where family ID was included in a model as a random intercept, with age and gender included as additional covariates. Analyses were firstly performed for each cohort separately and then combined using a fixed effects meta-analysis approach (R package *meta*, *metagen*(method = "FE")). Prior to analyses, glycan variables were all transformed to standard Normal distribution (mean=0, sd=1) by inverse transformation of ranks to Normality (R package "GenABEL", function *rnttransform*). Using rank transformed variables in analyses makes estimated effects of different glycans in different cohorts comparable as transformed glycan variables have the same standardized variance. False discovery rate was controlled using the Benjamini-Hochberg procedure (function *p.adjust*(method = "BH")). Data was analysed and visualized using R programming language (version 3.5.2). Differences in N-glycosylation between children with DS, including CRO1, and healthy children were visualized using principal components analysis (PCA). PCA was applied on directly measured IgG glycan peaks (GP1-GP24) using GraphPad Prism v9.2.0 PCA with standardized scale. Input was all individual GP1-GP24 values, unbiased. PCA was also applied on five derived glycan traits (G0, G1, G2, S and F) the levels of which were found to be significantly different between persons with DS and healthy controls in a large combined adult cohort.

Tables

Table 1. Characteristics of Down syndrome cohorts and healthy controls.

	France		Italy		UK	
	Controls N=109	DS N=98	Controls N=53	DS N=57	Controls N=42	DS N=53
Age (years) (median (range))	46 (22-67)	46 (30-67)	38 (22-66)	36 (22-66)	47 (22-82)	49 (22-73)
Sex (N) (female/male)	54/55	51/47	25/28	24/33	17/25	22/31
Autoimmune diseases (N)	0	34	0	28	0	25
Thyroid disease (N)	0	23	0	24	0	24
Dementia (N)	0	20	0	NA	0	13
Frequent infections (N)	0	15	0	16	0	7

N - number of samples/subjects

NA - data not available

Declarations

Acknowledgements

This work has been supported by the “Research Cooperability” Program of the Croatian Science Foundation funded by the European Union from the European Social Fund under the Operational Programme Efficient Human Resources 2014-2020 (Project PZS-2019-02-4277 to GL and DN). This work has been also supported in part by the European Structural and Investment funding for the ‘Croatian National Centre of Research Excellence in Personalized Healthcare’ (contract #KK.01.1.1.01.0010), ‘Centre of Competences in Molecular Diagnostics’ (contract #KK.01.2.2.03.0006), and the European Regional Development Fund grant ‘CardioMetabolic’ agreement (#KK.01.2.1.02.0321). DN was also funded by the Singapore Ministry of Education Academic Research Fund Tier 2 grants (2015-T2-1-023 & 2015-T2-2-119) and The Wellcome Trust Collaborative Award in Science 217199/Z/19/Z. the teams of AS, MT and DN also received funding from the Wellcome Trust “LonDownS Consortium” Strategic Funding Award (098330/Z/12/Z) (UK). AM is a Jérôme Lejeune Foundation fellow, funded by a Jérôme Lejeune Foundation Post-doctoral Fellowship. AS and ASR are also supported by funding from the Jérôme Lejeune Foundation that supported the DS cohorts in London and Paris. In addition, AS was supported by funding from the MRC (Medical Research Council grants MRC S011277/1, MR/S005145/1 (from Centres of Excellence in Neurodegeneration research) and MR/R024901/1 (from JPND). This work was also supported by Waterloo Foundation, Baily Thomas Charitable Fund, and Jérôme Lejeune Foundation (1901-1-2019b). The work of doctoral student HD has been supported by the “Young researchers' career development project – training of doctoral students” of the Croatian Science Foundation. We thank the

CRB-BioJeL biobank (<https://www.crb-institutlejeune.com/en/home/>), the LonDownS Consortium and the Italian biobank for providing samples. DM work has been supported by the Croatian Science Foundation project Orastem (IP-16-6-9451) and the European Union through the European Regional Development Fund, as the Scientific Centre of Excellence for Basic, Clinical and Translational Neuroscience under Grant Agreement No. KK.01.1.1.01.0007, project “Experimental and clinical research of hypoxic-ischemic damage in perinatal and adult brain”

Appendix 1

LonDownS Consortium, The Wellcome Trust, London, UK. The LonDownS Consortium principal investigators are: Andre Strydom, Department of Forensic and Neurodevelopmental Sciences, Institute of Psychiatry, Psychology and Neuroscience, King’s College London, London, UK and Division of Psychiatry, University College London, London, UK; Elizabeth Fisher and Frances Wiseman, Department of Neurodegenerative Disease, UCL Institute of Neurology, London, UK; Dean Nizetic, Blizard Institute, Barts and the London School of Medicine, Queen Mary, University of London, London, UK, and Lee Kong Chian School of Medicine, Nanyang Technological University, Singapore, Singapore; John Hardy, Reta Lila Weston Institute, Institute of Neurology, University College London, London, UK, and UK Dementia Research Institute at UCL, London, UK; Victor Tybulewicz, Francis Crick Institute, London, UK and Department of Medicine, Imperial College, London, UK; Annette Karmiloff-Smith (Birkbeck University of London) (deceased); Michael S. C. Thomas, Birkbeck University of London, London, UK; and Denis Mareschal, Birkbeck University of London, London, UK.

Author Contributions

G.L. and D.N. conceptualized the study. C.F., I.B., T.S., M.T., A.Str. and A-S.R. lead the clinical teams providing the samples and co-morbidities stratification, V.B., S.H., C.S., R.H., H.D’S, M.K. and Lj.O. obtained the primary samples; A.M., I.A., J.G., N.O’B. D.P. and D.M. processed the samples. A.C., J.J., M.P-B., A.Sla., H.D. and J.K. performed glycan analysis. F.V. and A.F. conducted statistical analysis. F.V., D.K. and J.K. produced the figures. F.V., D.K., A.Str., A-S.R., V.B., G.L., J.K. and D.N. interpreted the results. J.K. and D.N. wrote the first draft of the manuscript. G.L. critically *revised the initial draft of the manuscript*. A.C. helped to edit the manuscript. All authors reviewed and approved the final version of the manuscript.

Competing Interests statement

G.L. is the founder and owner of Genos Ltd, a private research organization that specializes in high-throughput glycomic analyses and has several patents in this field. A.C., F.V., J.J., M.P-B., A.Sla., H.D., A.F., D.P. and J.K. are employees of Genos Ltd.

References

1. Antonarakis, S. E. *et al.* Down syndrome. *Nat. Rev. Dis. Prim.* **6**, 1–20 (2020).
2. Epstein, C. J. 2001 William Allan award address from down syndrome to the 'Human' in 'Human Genetics'. *Am. J. Hum. Genet.* **70**, 300–313 (2002).
3. Wiseman, F. K. *et al.* A genetic cause of Alzheimer disease: Mechanistic insights from Down syndrome. *Nat. Rev. Neurosci.* **16**, 564–574 (2015).
4. Hithersay, R. *et al.* Association of Dementia with Mortality among Adults with Down Syndrome Older Than 35 Years. *JAMA Neurol.* **76**, 152–160 (2019).
5. Cuadrado, E. & Barrena, M. J. Immune dysfunction in Down's syndrome: Primary immune deficiency or early senescence of the immune system? *Clin. Immunol. Immunopathol.* **78**, 209–214 (1996).
6. da Silva, V. Z. M. *et al.* Bone mineral density and respiratory muscle strength in male individuals with mental retardation (with and without Down Syndrome). *Res. Dev. Disabil.* **31**, 1585–1589 (2010).
7. Komatsu, T. *et al.* Reactive oxygen species generation in gingival fibroblasts of Down syndrome patients detected by electron spin resonance spectroscopy. *Redox Rep.* **11**, 71–77 (2006).
8. Roizen, N. J. & Patterson, D. Down's syndrome. *Down's Syndr.* **361**, 1281–9 (2003).
9. Doran, E. *et al.* Down Syndrome, Partial Trisomy 21, and Absence of Alzheimer's Disease: The Role of APP. *J Alzheimers Dis.* **56**, 459–470 (2017).
10. Prasher, V. P. *et al.* Molecular mapping of Alzheimer-type dementia in Down's syndrome. *Ann. Neurol.* **43**, 380–383 (1998).
11. Head, E., Silverman, W., Patterson, D. & Lott, I. T. Aging and down syndrome. *Curr. Gerontol. Geriatr. Res.* **2012**, (2012).
12. Nižetić, D. & Groet, J. Tumorigenesis in Down's syndrome: Big lessons from a small chromosome. *Nat. Rev. Cancer* **12**, 721–732 (2012).
13. Busciglio, G. & Yankner, B. Apoptosis and increased generation of ROS in DS neurons in vitro. *Nature* **378**, 776–779 (1995).
14. Murray, A. *et al.* Isogenic induced pluripotent stem cell lines from an adult with mosaic Down Syndrome model accelerated neuronal ageing and neurodegeneration. *Stem Cells* **33**, 2077–2084 (2015).
15. Del Bo, R. *et al.* Down's syndrome fibroblasts anticipate the accumulation of specific ageing-related mtDNA mutations. *Ann. Neurol.* **49**, 137–8 (2001).

16. Druzhyna, N., Nair, R. G., Ledoux, S. P. & Wilson, G. L. Defective repair of oxidative damage in mitochondrial DNA in Down's syndrome. *Mutat. Res. - DNA Repair* **409**, 81–89 (1998).
17. Necchi, D. *et al.* Defective DNA repair and increased chromatin binding of DNA repair factors in Down syndrome fibroblasts. *Mutat. Res. - Fundam. Mol. Mech. Mutagen.* **780**, 15–23 (2015).
18. Raji, N. S. & Rao, K. S. Trisomy 21 and accelerated aging: DNA-repair parameters in peripheral lymphocytes of Down's syndrome patients. *Mech. Ageing Dev.* **100**, 85–101 (1998).
19. Amiel, A., Goldzak, G., Gaber, E. & Fejgin, M. D. Molecular cytogenetic characteristics of Down syndrome newborns. *J. Hum. Genet.* **51**, 541–547 (2006).
20. Zana, M. *et al.* Age-dependent oxidative stress-induced DNA damage in Down's lymphocytes. *Biochem. Biophys. Res. Commun.* **345**, 726–733 (2006).
21. Morawiec, Z. *et al.* DNA damage and repair in children with Down's syndrome. *Mutat. Res. - Fundam. Mol. Mech. Mutagen.* **637**, 118–123 (2008).
22. Thomas, P., Harvey, S., Gruner, T. & Fenech, M. The buccal cytome and micronucleus frequency is substantially altered in Down's syndrome and normal ageing compared to young healthy controls. *Mutat. Res. - Fundam. Mol. Mech. Mutagen.* **638**, 37–47 (2008).
23. Ishihara, K. *et al.* Increased lipid peroxidation in Down's syndrome mouse models. *J. Neurochem.* **110**, 1965–1976 (2009).
24. Wang, Y. *et al.* Hematopoietic Stem Cells from Ts65Dn Mice Are Deficient in the Repair of DNA Double-Strand Breaks. *Radiat. Res.* **185**, 630–637 (2016).
25. Hadi, E. *et al.* Telomere aggregates in trisomy 21 amniocytes. *Cancer Genet. Cytogenet.* **195**, 23–26 (2009).
26. Cobb, B. A. The history of IgG glycosylation and where we are now. *Glycobiology* **30**, 202–213 (2020).
27. Gudelj, I., Lauc, G. & Pezer, M. Immunoglobulin G glycosylation in aging and diseases. *Cell. Immunol.* **333**, 65–79 (2018).
28. Krištić, J. *et al.* Glycans are a novel biomarker of chronological and biological ages. *Journals Gerontol. - Ser. A Biol. Sci. Med. Sci.* **69**, 779–789 (2014).
29. Horvath, S. *et al.* Accelerated epigenetic aging in Down syndrome. *Aging Cell* **14**, 491–495 (2015).
30. Hanić, M., Lauc, G. & Trbojević-Akmačić, I. N-Glycan Analysis by Ultra-Performance Liquid Chromatography and Capillary Gel Electrophoresis with Fluorescent Labeling. *Curr. Protoc. Protein Sci.* **97**, 1–21 (2019).

31. Trbojević-Akmačić, I., Ugrina, I. & Lauc, G. Comparative Analysis and Validation of Different Steps in Glycomics Studies. *Methods Enzymol.* **586**, 37–55 (2017).
32. Petrović, T. *et al.* Composition of the immunoglobulin G glycome associates with the severity of COVID-19. *Glycobiology* cwa102. (2020).
33. Martin, T. C. *et al.* Decreased IgG core fucosylation, a player in antibody-dependent cell-mediated cytotoxicity, is associated with autoimmune thyroid diseases. *Mol Cell Proteomics* **19**, 774–792 (2020).
34. Cvetko, A. *et al.* Glycosylation alterations in multiple sclerosis show increased proinflammatory potential. *Biomedicines* **8**, 1–14 (2020).
35. Gudelj, I. *et al.* Low galactosylation of IgG associates with higher risk for future diagnosis of rheumatoid arthritis during 10 years of follow-up. *Biochim. Biophys. Acta - Mol. Basis Dis.* **1864**, 2034–2039 (2018).
36. Menni, C. *et al.* Glycosylation Profile of Immunoglobulin G Is Cross-Sectionally Associated with Cardiovascular Disease Risk Score and Subclinical Atherosclerosis in Two Independent Cohorts. *Circ. Res.* **122**, 1555–1564 (2018).
37. Vučković, F. *et al.* Association of systemic lupus erythematosus with decreased immunosuppressive potential of the IgG glycome. *Arthritis Rheumatol.* **67**, 2978–2989 (2015).
38. Mann, D. M. A. Alzheimer's disease and Down's syndrome. *Histopathology* **13**, 125–137 (1988).
39. Chistiakov, D. Down syndrome and coexistent autoimmune diseases. *J. Appl. Biomed.* **5**, 71–76 (2007).
40. Štambuk, J. *et al.* Global variability of the human IgG glycome. *Aging (Albany, NY)*. **12**, 15222–15259 (2020).
41. Franceschi, C. *et al.* Accelerated bio-cognitive aging in Down syndrome: State of the art and possible deceleration strategies. *Aging Cell* **18**, 1–11 (2019).
42. Delabar, J. M. *et al.* Molecular mapping of twenty-four features of Down syndrome on chromosome 21. *European journal of human genetics: EJHG* **1**, 114–124 (1993).
43. Korenberg, J. R. *et al.* Molecular definition of a region of chromosome 21 that causes features of the down syndrome phenotype. *Am. J. Hum. Genet.* **47**, 236–246 (1990).
44. Fumagalli, M. & d'Adda di Fagagna, F. SASPense and DDRama in cancer and ageing. *Nat. Cell Biol.* **11**, 921–923 (2009).
45. Shapiro, B. L. Down Syndrome-A Homeostasis. *Am J Med Genet* **14**, 241–269 (1983).

46. Antonarakis, S. E., Lyle, R., Dermitzakis, E. T., Reymond, A. & Deutsch, S. Chromosome 21 and Down syndrome: From genomics to pathophysiology. *Nat. Rev. Genet.* **5**, 725–738 (2004).
47. Jenkins, E. C. *et al.* Increased low-level chromosome 21 mosaicism in older individuals with Down syndrome. *Am. J. Med. Genet.* **68**, 147–151 (1997).
48. Percy, M. E. *et al.* Age-associated chromosome 21 loss in Down syndrome: Possible relevance to mosaicism and Alzheimer disease. *Am. J. Med. Genet.* **45**, 584–588 (1993).
49. Lightfoot, D. A. & Höög, C. Low level chromosome instability in embryonic cells of primary aneuploid mice. *Cytogenet. Genome Res.* **107**, 95–98 (2004).
50. Reish, O., Regev, M., Kanesky, A., Girafi, S. & Mashevich, M. Sporadic aneuploidy in PHA-stimulated lymphocytes of trisomies 21, 18, and 13. *Cytogenet. Genome Res.* **133**, 184–189 (2011).
51. Fujita, H. *et al.* Premature aging syndrome showing random chromosome number instabilities with CDC20 mutation. *Aging Cell* **19**, 1–13 (2020).
52. Kazuki, Y. *et al.* A non-mosaic transchromosomic mouse model of down syndrome carrying the long arm of human chromosome 21. *Elife* **9**, 1–29 (2020).
53. O'Doherty, A. *et al.* An Aneuploid Mouse Strain Carrying Human Chromosome 21 with Down Syndrome Phenotypes. *Science (80-)*. **309**, 2033–2037 (2005).
54. Busciglio, J. *et al.* Altered metabolism of the amyloid β precursor protein is associated with mitochondrial dysfunction in Down's syndrome. *Neuron* **33**, 677–688 (2002).
55. De Haan, J. B. *et al.* Elevation in the ratio of Cu/Zn-superoxide dismutase to glutathione peroxidase activity induces features of cellular senescence and this effect is mediated by hydrogen peroxide. *Hum. Mol. Genet.* **5**, 283–292 (1996).
56. Adorno, M. *et al.* Usp16 contributes to somatic stem-cell defects in Down's syndrome. *Nature* **501**, 380–384 (2013).
57. Guard, S. E. *et al.* The nuclear interactome of DYRK1A reveals a functional role in DNA damage repair. *Sci. Rep.* **9**, 1–12 (2019).
58. Menon, R. *et al.* DYRK1A regulates the recruitment of 53BP1 to the sites of DNA damage in part through interaction with RNF169. *Cell Cycle* **18**, 531–551 (2019).
59. Roewenstrunk, J. *et al.* A comprehensive proteomics-based interaction screen that links DYRK1A to RNF169 and to the DNA damage response. *Sci. Rep.* **9**, 1–14 (2019).
60. Borelli, V. *et al.* Plasma N-Glycome Signature of Down Syndrome. *J. Proteome Res.* **14**, 4232–4245 (2015).

61. Relja, A. *et al.* Nut consumption and cardiovascular risk factors: A cross-sectional study in a mediterranean population. *Nutrients* **9**, 1–20 (2017).
62. Rudan, I. *et al.* '10 001 Dalmatians:' Croatia Launches Its National Biobank. *Croat. Med. J.* **50**, 4–6 (2009).
63. Dagostino, C. *et al.* Validation of standard operating procedures in a multicenter retrospective study to identify-omics biomarkers for chronic low back pain. *PLoS One* **12**, (2017).
64. Verdi, S. *et al.* TwinsUK: The UK Adult Twin Registry Update. *Twin Res. Hum. Genet.* **22**, 523–529 (2019).
65. Andrew, T. *et al.* Are twins and singletons comparable? A study of disease-related and lifestyle characteristics in adult women. *Twin Res.* **4**, 464–477 (2001).
66. Pezer, M. *et al.* Effects of allergic diseases and age on the composition of serum IgG glycome in children. *Sci. Rep.* **6**, 1–10 (2016).
67. Lyle, R. *et al.* Genotype-phenotype correlations in Down syndrome identified by array CGH in 30 cases of partial trisomy and partial monosomy chromosome 21. *Eur. J. Hum. Genet.* **17**, 454–466 (2009).
68. Ugrina, I., Campbell, H. & Vučković, F. Laboratory Experimental Design for a Glycomic Study. in *Methods Mol Biol.* (eds. Lauc, G. & Wuhrer, M.) 13–19 (Humana Press, New York, NY, 2017).
69. Pucic, M. *et al.* High throughput isolation and glycosylation analysis of IgG-variability and heritability of the IgG glycome in three isolated human populations. *Mol Cell Proteomics* **10**, M111.010090 (2011).

Figures

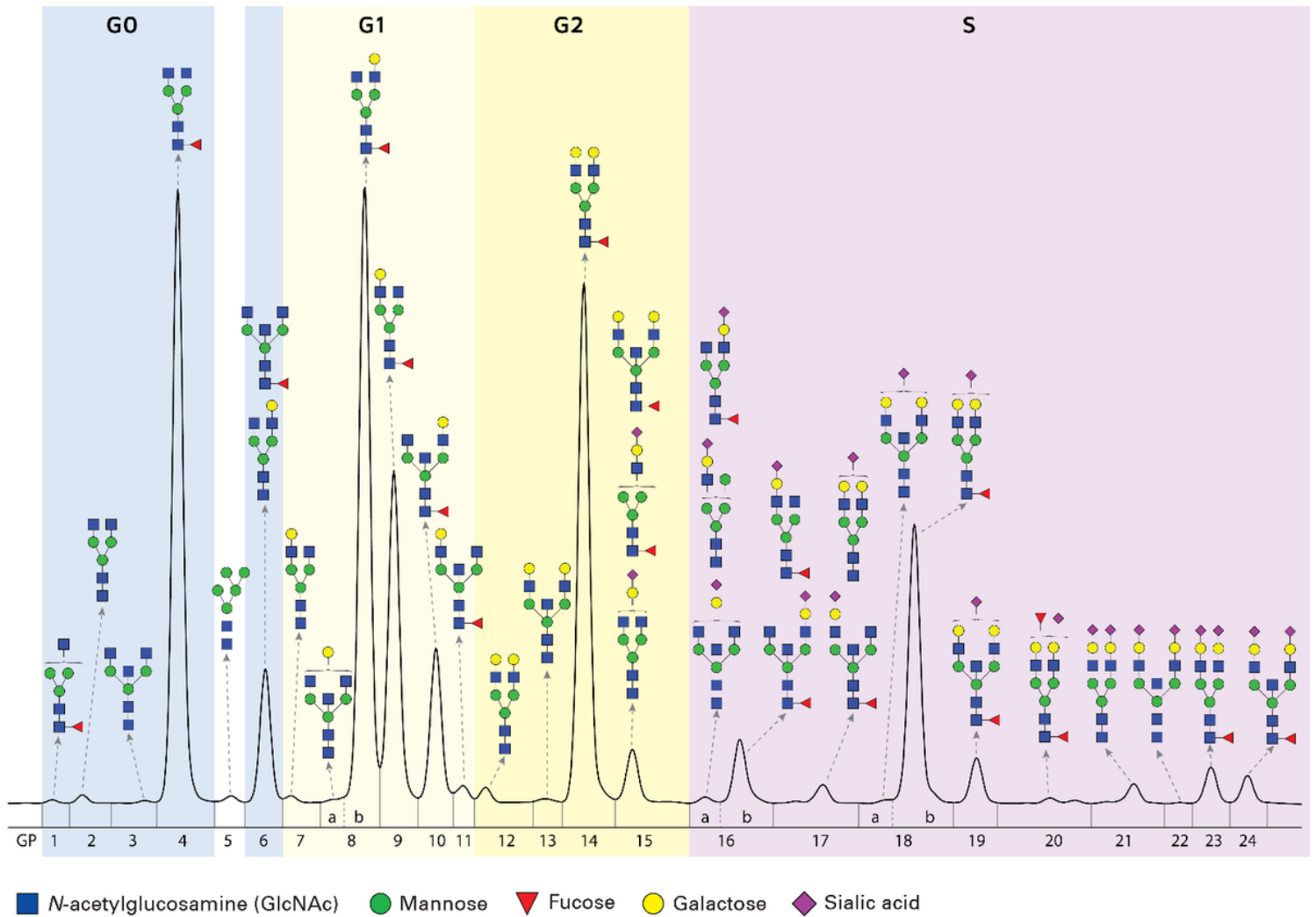


Figure 1

Chromatographic profile of N-glycans released from immunoglobulin G (IgG) isolated from human plasma. IgG glycans are separated into 24 peaks labelled GP1-GP24. Majority of individual peaks correspond to a single glycan structure. In case of multiple glycan structures per glycan peak (GP), the uppermost one is the most abundant structure in the corresponding peak and the lower ones are minor glycan structures. GP – glycan peak, G0 – IgG glycans without galactose, G1 – IgG glycans with one galactose, G2 – IgG glycans with two galactoses, S – IgG glycans with sialic acid(s).

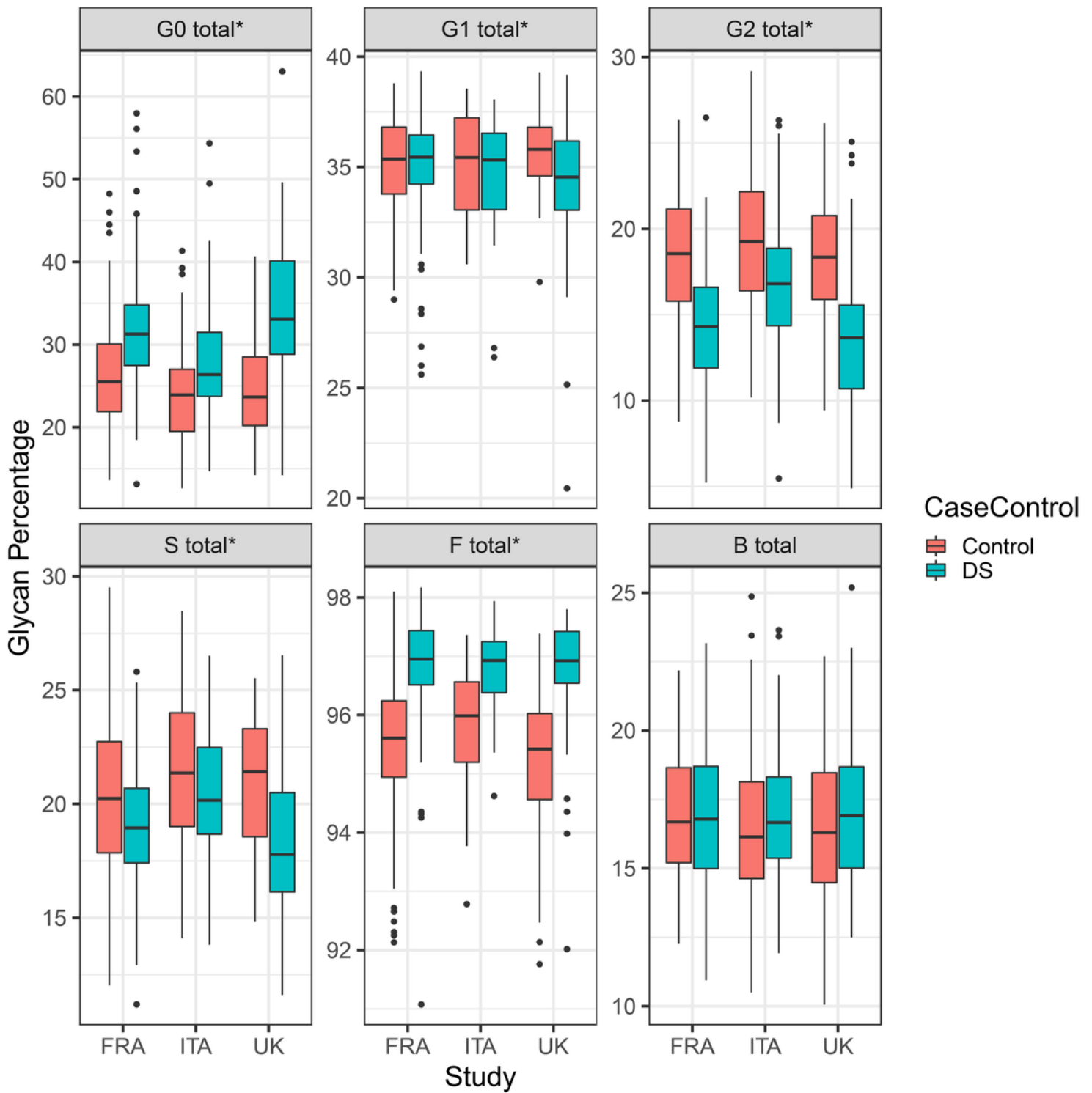


Figure 2

Levels of six derived IgG glycan traits in persons with Down syndrome (DS) and in healthy controls shown separately for three cohorts of adults with Down syndrome from France (FRA), Italy (ITA) and the UK. G0 total – sum of IgG glycans without galactose, G1 total – sum of IgG glycans with one galactose, G2 total – sum of IgG glycans with two galactoses, S total – sum of IgG glycans with sialic acid(s), F total – sum of IgG glycans with core fucose, B total – sum of IgG glycans with bisecting GlcNAc. Data are shown as box plots. Each box represents the 25th to 75th percentiles (the interquartile range (IQR)).

Lines inside the boxes represent the median. Lines outside the boxes indicate data within 1.5 x IQR from the 25th and 75th percentiles. Black dots indicate outliers. Asterisk * sign next to the derived trait name indicates statistically significant differences ($p < 0.05$, meta-analysis) between DS individuals and healthy controls (additional information is available in **Supplementary Table 1**).

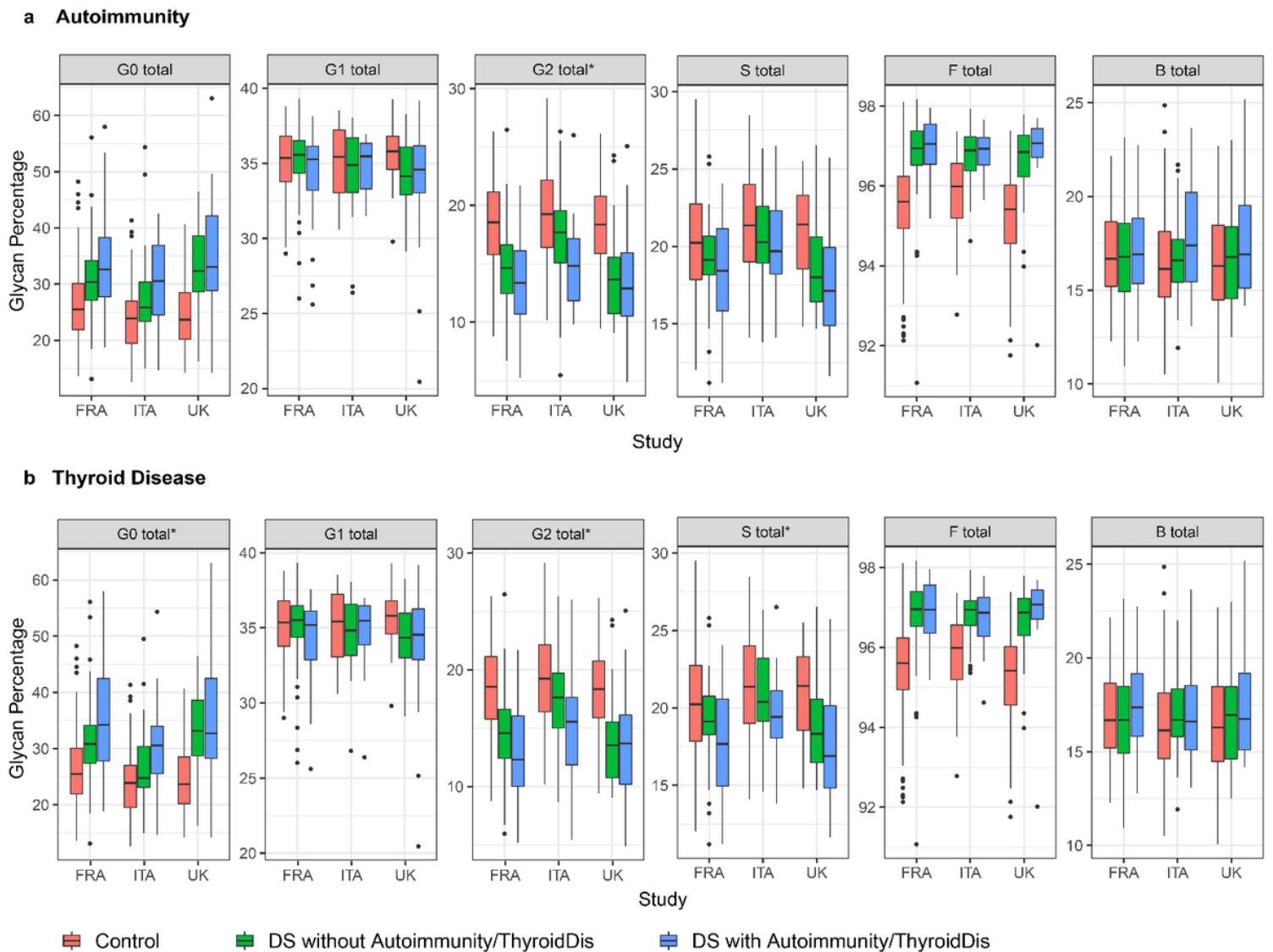


Figure 3

Comparison of levels of derived IgG glycan traits between healthy control individuals, persons with Down syndrome without autoimmune conditions and persons with Down syndrome with autoimmune conditions. **a**, Comparison between controls and persons with DS with or without any type of autoimmune disease; **b**, Comparison between controls and persons with DS with or without *autoimmune thyroid disease*. G0 total – sum of IgG glycans without galactose, G1 total – sum of IgG glycans with one galactose, G2 total – sum of IgG glycans with two galactoses, S total – sum of IgG glycans with sialic acid(s), F total – sum of IgG glycans with core fucose, B total – sum of IgG glycans with bisecting

GlcNAc. Data are shown as box plots. Each box represents the 25th to 75th percentiles (the interquartile range (IQR)). Lines inside the boxes represent the median. Lines outside the boxes indicate data within 1.5 x IQR from the 25th and 75th percentiles. Black dots indicate outliers. Asterisk * sign next to the derived trait name indicates statistically significant differences (p <0.05, meta-analysis) between DS individuals with and without autoimmune conditions (additional information is available in **Supplementary Table 4**)

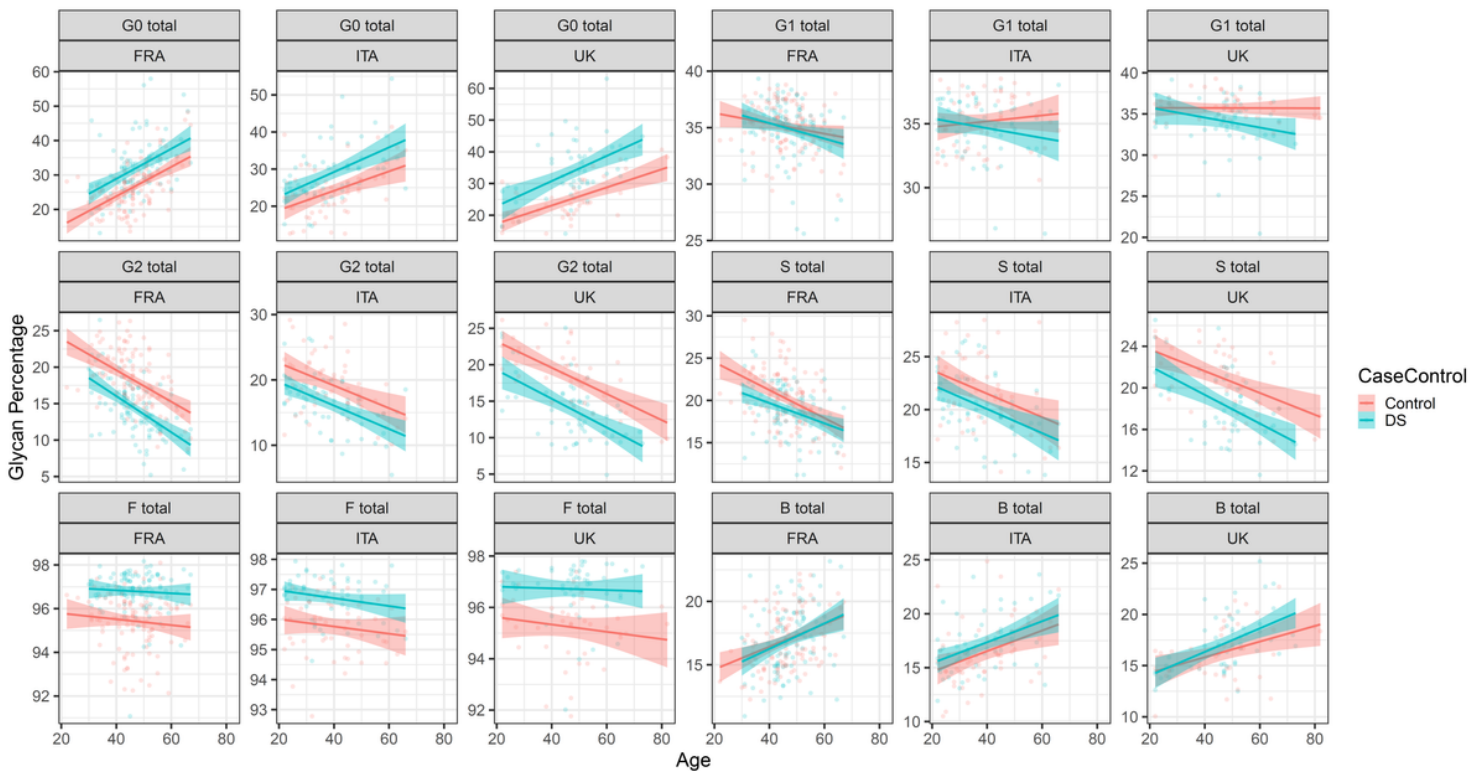


Figure 4

Relationship between age and levels of six derived IgG glycan traits in persons with Down syndrome (DS) and in healthy controls shown separately for three cohorts of adults with Down syndrome from France (FRA), Italy (ITA) and the UK. Blue and red lines represent fitted local regression models for the control and DS data, respectively. The shaded region is a 95% confidence interval on the fitted values. Individual subject data points are presented on the background. G0 total – sum of IgG glycans without galactose, G1 total – sum of IgG glycans with one galactose, G2 total – sum of IgG glycans with two galactoses, S total – sum of IgG glycans with sialic acid(s), F total – sum of IgG glycans with core fucose, B total – sum of IgG glycans with bisecting GlcNAc. Trendline equations: G0 FRA control: $y=0.43x + 6.72$; G0 FRA DS: $y=0.44x + 11.42$; G0 ITA control: $y=0.26x + 13.74$; G0 ITA DS: $y=0.33x + 15.96$; G0 UK control: $y=0.29x + 11.63$; G0 UK DS: $y=0.40x + 14.92$; G2 FRA control: $y=-0.22x + 28.25$; G2 FRA DS: $y=-0.25x + 25.96$; G2 ITA control: $y=-0.17x + 26.04$; G2 ITA DS: $y=-0.18x + 23.23$; G2 UK control: $y=-0.18x + 26.79$; G2 UK DS: $y=-0.20x + 23.22$.

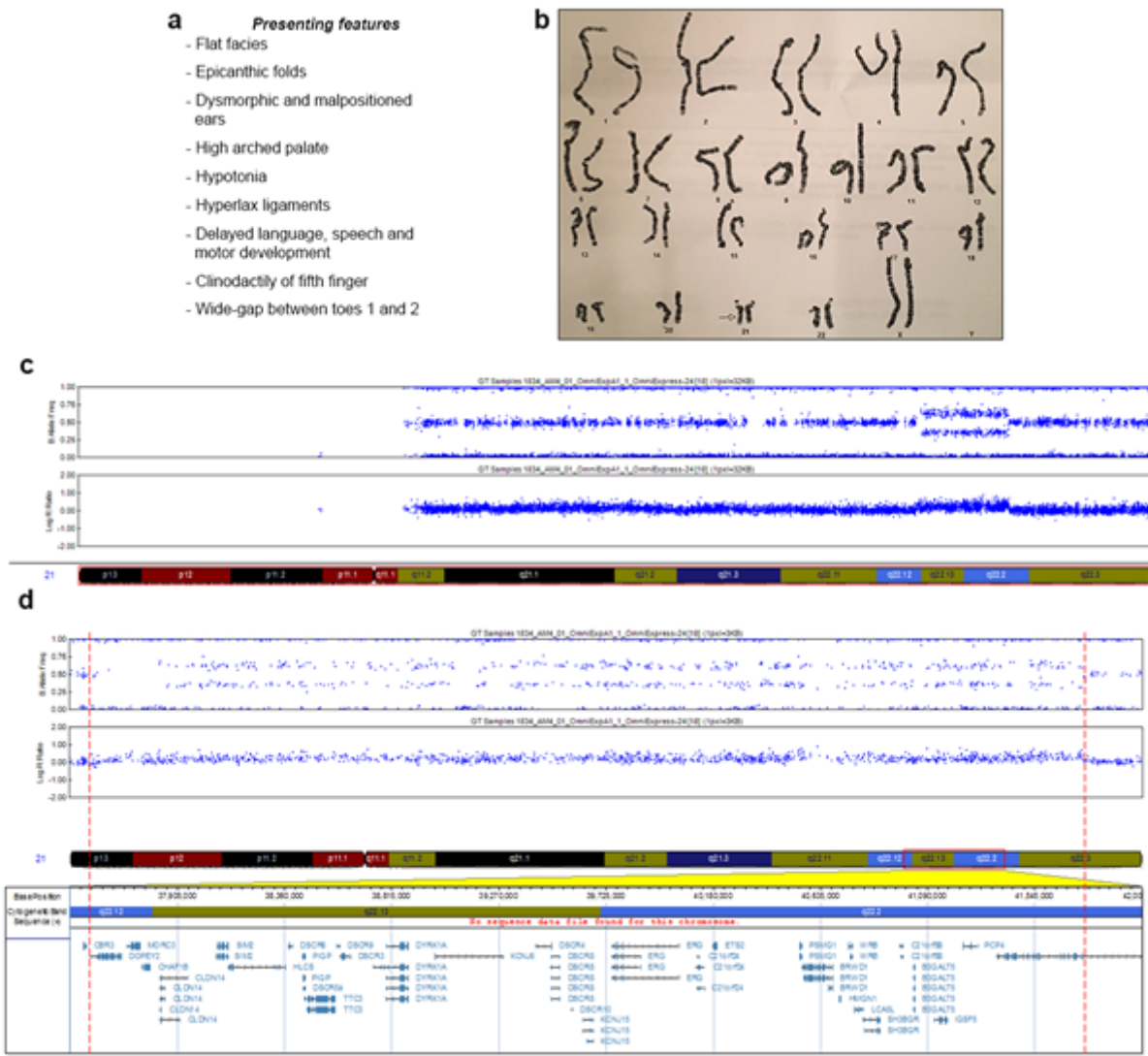


Figure 5

Clinical, cytogenetic and molecular characterization of a child (codenamed CRO1) with clinical features of Down syndrome and a partial trisomy 21 caused by a segmental duplication of 31 genes. **a**, Clinical aspects within the spectrum of DS-phenotypic features present upon examination of the CRO1 child. Full list of present and absent features is shown in **Supplementary Table 8**. **b**, Full karyotype of the CRO1 child. Normal number of chromosomes, with a small duplication in the 21q22 region (arrow). **c,d**, SNP array analysis from CRO1 genomic DNA for human chromosome 21. A red box around the chromosome icon indicates the region of the chromosome displayed for the corresponding SNP data. **c**, B-allele and LogR ratio are shown for the entire length of chromosome 21, showing an approximate 4 Mbp duplication in the q22.12 to q22.2 region. **d**, B-allele and LogR ratio are shown for chromosome 21 coordinates 37,450,000 - 42,000,000 (GRCh37) which encompasses the entire duplication along with the proximal and distal disomic SNPs. The gene content of the region is noted below the figure. Examining

both B-allele frequency and the increase in LogR ratio, the duplication starts in the region of *DOPEY2* and ends in *DSCAM*, as indicated by red dashed lines.

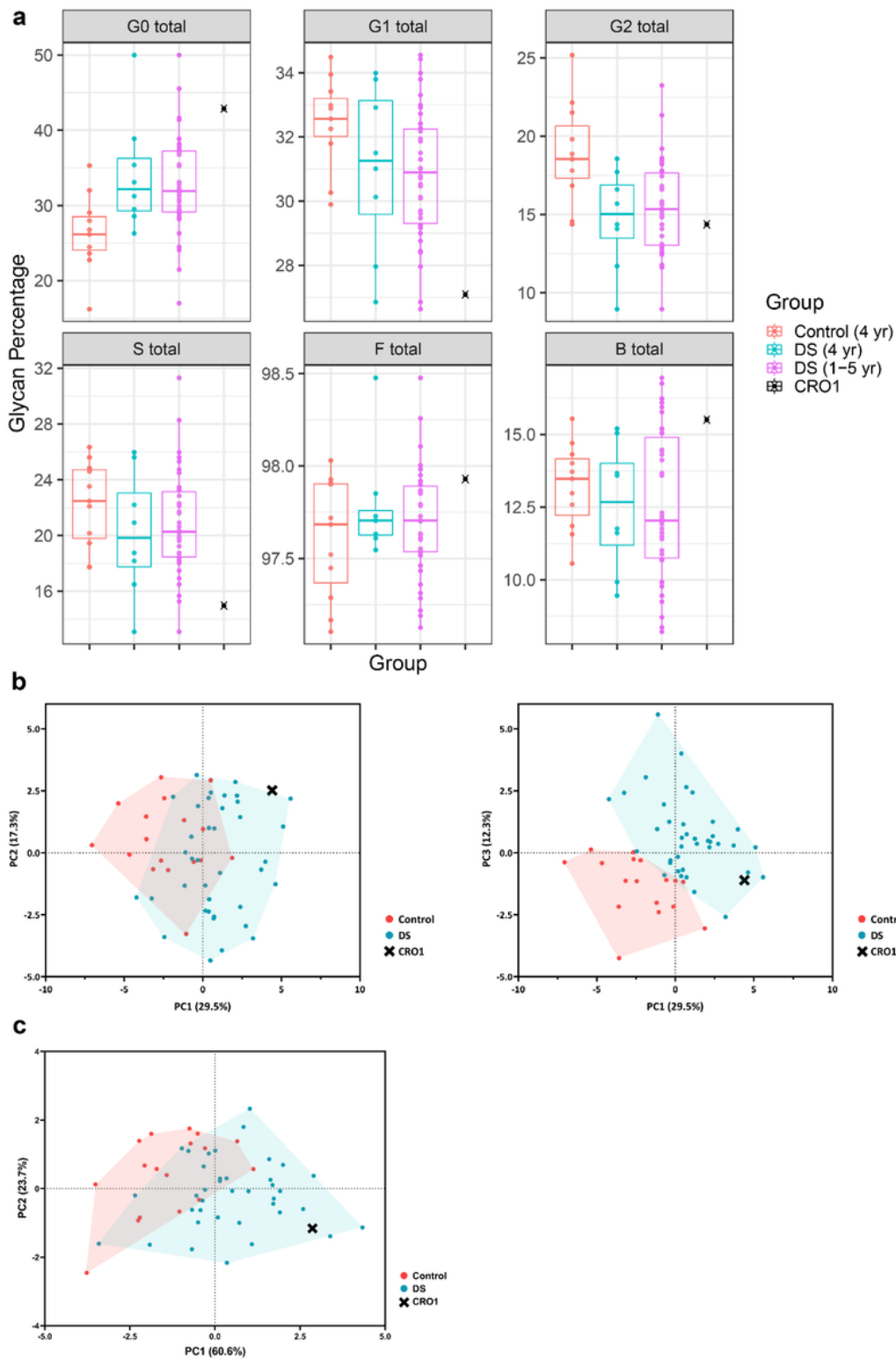


Figure 6

IgG glycosylation in children with Down syndrome including a child with segmental trisomy 21. a, Levels of six derived IgG glycan traits in around 4-year-old children with Down syndrome (DS) from the UK

cohort, in 4-year-old healthy children, in other DS children aged 1 to 5 years, and in CRO1 child with segmental trisomy 21. G0 total – sum of IgG glycans without galactose, G1 total – sum of IgG glycans with one galactose, G2 total – sum of IgG glycans with two galactoses, S total – sum of IgG glycans with sialic acid(s), F total – sum of IgG glycans with core fucose, B total – sum of IgG glycans with bisecting GlcNAc. Data are shown as box plots with individual data points. Each box represents the 25th to 75th percentiles (IQR). Lines inside the boxes represent the median. Lines outside the boxes indicate data within 1.5 x IQR from the 25th and 75th percentiles. Each dot represents one child. CRO1 child is marked as single black cross. **b**, Principal component analysis (PCA) displaying differences in IgG glycosylation between DS children and healthy children: PC1 vs PC2 plot (left) and PC1 vs PC3 plot (right). PCA positioned CRO1 child with segmental trisomy 21 (marked as a black cross) within the DS sample cluster. Each dot represents one child. n (children with DS) = 38 + CRO1 child, n (euploid children) = 17. PCA was performed on directly measured IgG glycan peaks (GP1-GP24). **c**, PCA on G0, G1, G2, S and F derived IgG glycan traits values.

Supplementary Files

This is a list of supplementary files associated with this preprint. Click to download.

- [Cindricetal.IgGglycosylationinDownsyndromeSupplementarydata.docx](#)